



Contents lists available at ScienceDirect

## Bioorganic &amp; Medicinal Chemistry

journal homepage: [www.elsevier.com/locate/bmc](http://www.elsevier.com/locate/bmc)

# Halogenated trimethoprim derivatives as multidrug-resistant *Staphylococcus aureus* therapeutics

Napon Nilchan<sup>a</sup>, Wanida Phetsang<sup>a</sup>, Taechin Nowwarat<sup>a</sup>, Soraya Chaturongakul<sup>b,c</sup>,  
Chutima Jiarpinitnun<sup>a,\*</sup>

<sup>a</sup> Department of Chemistry and Center for Innovation in Chemistry (PERCH-CIC), Faculty of Science, Mahidol University, Rama VI Road, Bangkok 10400, Thailand

<sup>b</sup> Department of Microbiology, Faculty of Science, Mahidol University, Rama VI Road, Bangkok 10400, Thailand

<sup>c</sup> Center for Emerging Bacterial Infections, Faculty of Science, Mahidol University, Rama VI Road, Bangkok 10400, Thailand

## ARTICLE INFO

This manuscript is dedicated to Professor Laura L. Kiessling in celebration of her career contributions to organic chemistry.

## Keywords:

Trimethoprim  
Methicillin resistant *Staphylococcus aureus*  
Halogenation

## ABSTRACT

Incorporation of halogen atoms to drug molecule has been shown to improve its properties such as enhanced in membrane permeability and increased hydrophobic interactions to its target. To investigate the effect of halogen substitutions on the antibacterial activity of trimethoprim (TMP), we synthesized a series of halogen substituted TMP and tested for their antibacterial activities against global predominant methicillin resistant *Staphylococcus aureus* (MRSA) strains. Structure-activity relationship analysis suggested a trend in potency that correlated with the ability of the halogen atom to facilitate in hydrophobic interaction to saDHFR. The most potent derivative, iodinated trimethoprim (TMP-I), inhibited pathogenic bacterial growth with MIC as low as 1.25 µg/mL while the clinically used TMP derivative, diaveridine, showed resistance. Similar to TMP, synergistic studies indicated that TMP-I functioned synergistically with sulfamethoxazole. The simplicity in the synthesis from an inexpensive starting material, vanillin, highlighted the potential of TMP-I as antibacterial agent for MRSA infections.

## 1. Introduction

*Staphylococcus aureus* (*S. aureus*) is an opportunistic Gram-positive bacterial pathogen accounted for one of the major public health problems worldwide.<sup>1,2</sup> The key concern of *S. aureus* infection is due to rapid development of antibiotic resistance that could complicate the treatment. Methicillin-resistant *S. aureus* (MRSA), in particular, acquires resistance to commonly used β-lactam antibiotics such as penicillin. Since its first report in 1961, MRSA infection has now been considered endemic. The impact of infection is substantial. In the United States alone, MRSA infection results in an estimate of 19,000 deaths in addition to \$3–4 billion antibiotics and hospitalization cost annually.<sup>3</sup> Hence, the developments of effective antibiotics and strategies to combat resistance bacteria are called for.

The combination of antibiotics has been one of the treatment choices for infections that caused by bacteria with high mutation rate.<sup>4,5</sup> Combination of trimethoprim (TMP)-sulfamethoxazole (SMZ) or co-trimethoxazole is a successful example of combination antibiotic therapy, recommended as first-line of treatments for urinary tract infections, soft tissue infections, and MRSA infection, particularly community-associated MRSA (CA-MRSA). TMP and SMZ are potent and selective inhibitors of two key enzymes in the folate biosynthetic

pathway, namely dihydrofolate reductase (DHFR) and dihydropteroate synthase (DHPS), respectively.<sup>6,7</sup> Disruption of folate pathways inhibits productions of key intermediates for DNA nucleoside and protein syntheses, eventually leading to cell death. Folate pathway has been widely focused as therapeutic target for antibacterial agent development due to the difference in folate sources in pathogens and in mammals.<sup>8</sup> Bacteria solely depend on the biosynthesis of folate pathway while mammalian host could uptake folates from nutrients. Therefore, blocking sequential steps in the folate synthesis pathway by SMZ and TMP could lead to death of pathogens and not perturb the mammalian host. TMP and SMZ have been shown to function synergistically, resulting in dramatic enhancement in antibacterial activity.<sup>9</sup> However, the rises of SMZ-resistance, TMP-resistance, and resistance to the combination therapy have called for new antibacterial agents.<sup>10,11</sup>

RAB1, a phthalazine analogue of TMP, was reported as a DHFR inhibitor that exhibited broad spectrum activity with exceptional effectiveness against *S. aureus* and MRSA (Fig. 1).<sup>12</sup> The reported X-ray crystal structure of *S. aureus* DHFR (saDHFR) with trimethoprim and with RAB1 suggested a unique shallow surface cavity that could be exploited in drug development.<sup>12</sup> The co-crystal complex structure with DHFR also indicated that the F98Y mutation<sup>13</sup>, which commonly found

\* Corresponding author.

E-mail address: [chutima.jia@mahidol.ac.th](mailto:chutima.jia@mahidol.ac.th) (C. Jiarpinitnun).

<https://doi.org/10.1016/j.bmc.2018.05.019>

Received 28 February 2018; Received in revised form 10 May 2018; Accepted 13 May 2018  
0968-0896/ © 2018 Elsevier Ltd. All rights reserved.

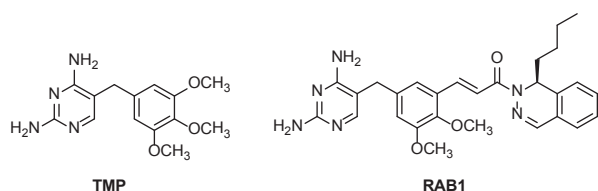


Fig. 1. Structure of TMP and TMP derivative RAB1.

in TMP-resistance strains, has minimal effects on saDHFR binding to RAB1, highlighting the shallow surface cavity of saDHFR as an excellent target for MRSA therapeutic development.

The unique shallow surface cavity of saDHFR contains the electron-rich sites from side chains and backbones of amino acids; therefore, we envisioned that incorporation of halogens into DHFR inhibitor structure may allow better interactions of the inhibitor with these surrounding electron-rich via halogen bonds interactions. Halogens could facilitate in the non-directional hydrophobic interactions that could enhance the binding contact.<sup>14</sup> Here in, we investigated the effect of halogens substitution on the antibacterial activity of TMP against *S. aureus* and MRSA.

## 2. Results and discussion

### 2.1. Chemistry

A series of halogenated derivatives of TMP—chlorinated-, brominated-, and iodinated- (abbreviated as TMP-Cl, TMP-Br, and TMP-I, respectively)—were synthesized. The syntheses were based on previously reported method as shown in Scheme 1.<sup>15</sup> In brief, an inexpensive commercially available vanillin was used as a starting material to undergo halogenation with various halogen sources. *N*-halosuccinimides such as *N*-chlorosuccinimide (NCS) and *N*-bromosuccinimide (NBS) were used for chlorination and bromination, respectively. The desired products **1a** and **1b** were obtained in moderate to high yield. For the electrophilic aromatic iodination of vanillin, we employed potassium iodide (KI) as the iodine source and the common household bleach solution as an oxidizing agent. 5-iodovanillin (**1c**) was obtained in excellent yield. Subsequently, the halogenated vanillin (**1a–1c**) was subjected to *o*-methylation reaction with methyl iodide (MeI) in the presence of tetrabutylammonium iodide (TBAI). Compound **2a–2c** were obtained in 96–98% yield. Condensation of the halogenated dimethoxy benzaldehyde adduct (**2a–2c**) with 3-morpholinopropionitrile using sodium methoxide in DMSO afforded alkene product, which were sequentially cyclized by treating with a guanidine hydrochloride to yield the corresponding halogenated derivatives of TMP in moderate yield (47–60%). 5-(3,4-dimethoxybenzyl)pyrimidine-

2,4-diamine), commonly known as diaveridine, of which a hydrogen atom was in place of a halogen, was also prepared for antibacterial activity comparison. The synthesis of diaveridine was achieved via a similar methodology using commercially available 3,4-dimethoxybenzaldehyde. All compounds were purified and characterized via nuclear magnetic spectroscopy and mass spectroscopy, as reported in the experimental section.

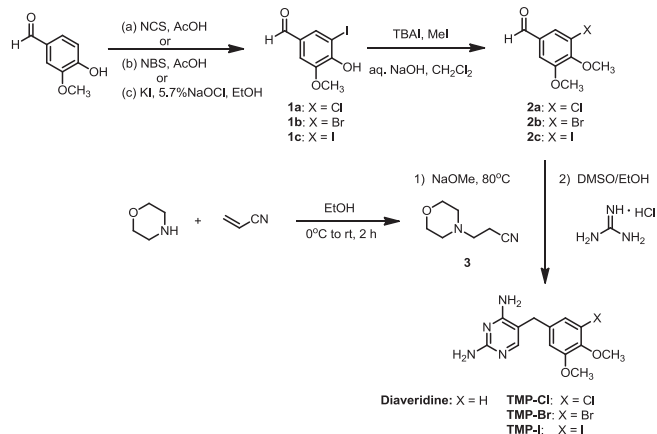
### 2.2. Susceptibility testing

All trimethoprim derivatives—TMP-Cl, TMP-Br, TMP-I, TMP, and diaveridine—were subjected to susceptibility assays against methicillin susceptible *S. aureus* (MSSA) control strains (ATCC25923 and ATCC29213), global predominant CA-MRSA PFGE strain USA300 (SF8300), and highly resistant hospital associated-MRSA (HA-MRSA) strain COL. Rapid transmission and resistance towards antibiotics of MRSA USA300 and COL strains lead to global healthcare problem.<sup>16,17</sup> Hence, the effective antibiotics against these pathogenic strains are searched for.

The synthesized compounds were first quantitatively screened for their ability to inhibit growth of pathogenic bacteria via disk diffusion assay. We tested all compounds at 5  $\mu$ g as recommended by Clinical and Laboratory Standards Institute (CLSI) for TMP.<sup>18</sup> The conventional antibiotic diaveridine exhibited incomplete inhibition zone when tested with MRSA USA300 and no inhibition zone when tested with COL strain. The results suggested that CA-MRSA USA300 and HA-MRSA strain COL are diaveridine-resistant. TMP resulted in complete inhibition zone in the range of > 16 mm (disk diffusion breakpoint for susceptibility suggested by CLSI) when tested with MSSA ATCC25923 and CA-MRSA; however, the results with HA-MRSA strain COL showed incomplete inhibition zone. Similar to TMP, all halogenated derivatives could completely inhibit growth of MSSA and CA-MRSA strain USA300 but incompletely inhibit HA-MRSA strain COL. Among halogenated series, TMP-I showed the highest inhibition zone (> 20 mm), followed by TMP-Br and TMP-Cl respectively. The trend is consistently observed in all three strains tested (Table 1).

With regards to chemical structures, the difference between diaveridine, TMP, and our synthesized halogenated TMP derivatives are subtle, only at *meta*-position of the benzene ring. However, this small difference in structure leads to significant change in the antibacterial activity. Replacing -H of diaveridine with electron donating -OMe moiety or with -halogens group at *meta*-position could significantly enhance the antibacterial activity, as evidently shown in > 15 mm inhibition zone in TMP and halogenated derivatives and < 9 mm in diaveridine. The results suggested that substitution at this particular position could change the antibacterial activity outcome.

All compounds were subjected to microdilution assay to quantitatively evaluate their antibacterial activity against MSSA and MRSA. The results are shown in Table 1. The minimum inhibitory concentration (MIC) and minimum bactericidal concentration (MBC) determined from microdilution assay also suggested similar trend in antibacterial potency correlated to the extents of inhibition zone observed in disk diffusion assay. The substituent at *meta*-position of the benzene ring was suggested key for MSSA and MRSA growth inhibitory activity. MSSA ATCC29213 showed susceptibility to all TMP derivatives while HA-MRSA COL strain exhibited resistant to diaveridine as its MIC was clearly above the breakpoint of 5  $\mu$ g/mL suggested by CLSI.<sup>18</sup> The potency of diaveridine was noticeably less potent (approximately 4-folds) in all strains tested. When substituted hydrogen atom at *meta*-position of diaveridine with halogens, the antibacterial potency against MSSA and MRSA strains were enhanced. All strains showed susceptibility to our synthesized halogenated derivatives (TMP-Cl, TMP-Br, and TMP-I). Interestingly, substitution with iodide led to the most potent *S. aureus* growth inhibitor analogue, even more active than the parent antibiotics TMP. Substitution with smaller halogens such as bromine and chlorine resulted in less active growth inhibitors. As clearly shown when tested



Scheme 1. Syntheses of halogenated TMP derivatives.

**Table 1**  
Antibacterial activities of TMP derivatives determined by disk diffusion<sup>a</sup> and microdilution susceptibility test.<sup>b</sup>

Compounds	Diameter of Inhibition zones (mm)			MIC ( $\mu\text{g/mL}$ )			MBC ( $\mu\text{g/mL}$ )			IC <sub>50</sub> ( $\mu\text{M}$ )
	ATCC25923	SF8300	COL	ATCC29213	SF8300	COL	ATCC29213	SF8300	COL	
diaveridine	8.81 $\pm$ 0.56	6 (++)	6	5	5	10	5	10	20	> 1000
TMP	20.19 $\pm$ 0.94	22.80 $\pm$ 0.92	6 (++)	1.25	1.25	5	1.25	2.5	10	–
TMP-Cl	15.06 $\pm$ 0.60	18.11 $\pm$ 0.61	6 (+)	1.25	2.5	5	1.25	2.5	10	467
TMP-Br	17.37 $\pm$ 0.93	20.39 $\pm$ 0.83	6 (++)	1.25	1.25	5	1.25	1.25	5	321
TMP-I	21.01 $\pm$ 0.03	22.82 $\pm$ 0.62	6 (++)	1.25	1.25	2.5	1.25	1.25	5	266

<sup>a</sup> 5  $\mu\text{g}$  of test compounds in DMSO were used for disk diffusion testing. At least three independent experiments were performed and the average diameters of complete inhibition zones were reported with standard errors. Whatman disk has a diameter of 6 mm; therefore, average inhibition zone of 6 mm indicates inability to inhibit growth. Incomplete inhibition zones were defined as +, ++, and +++, depending on the thickness of bacterial growth visualized. The incompleteness of +++ was given to a zone with the least thickness of bacterial growth, suggesting near completion of the inhibition zone. Meanwhile, + was given to that appeared to be more in thickness, suggesting near resistance.

<sup>b</sup> Each compound was 2-fold diluted based on its stock concentration.

against highly resistant HA-MRSA COL strain, TMP-I was the most potent among all the derivatives with MIC of 2.5  $\mu\text{g/mL}$ ; other halogenated derivatives and even the clinically used TMP resulted in MIC at the borderline susceptibility of 5  $\mu\text{g/mL}$ . Noticeably, they still resulted in better activity than diaveridine.

The synthesized TMP derivatives were subjected to cytotoxicity experiments with A549 cells. The IC<sub>50</sub> values of TMP-Cl, TMP-Br, and TMP-I were 467  $\mu\text{M}$ , 321  $\mu\text{M}$ , and 266  $\mu\text{M}$ , respectively. Even though these halogen-containing adducts exhibited higher toxicity than diaveridine (IC<sub>50</sub> > 1000  $\mu\text{M}$ ), their IC<sub>50</sub> values were significantly above their MIC and MBC values, suggesting that these compounds potentially would not be toxic to treated cells at the concentrations required for inhibiting growth or killing the pathogen.

To better understand the trend in potency observed, we performed molecular docking of the halogen-substituted derivatives with saDHFR using Schrödinger Maestro suites (Schrödinger suites 2017-4). The binding was compared to the binding of TMP and diaveridine, known inhibitors of DHFR. The structures of all compounds were constructed from TMP structure and their geometries were subsequently optimized using LigPrep in Schrödinger program suite. The structure of *S. aureus* DHFR was obtained from Protein Data Bank (PDB: 2W9H). The binding modes of halogenated TMP derivatives in the binding site of saDHFR were evaluated using Glide dock in standard precision (SP) with core constraints based on co-crystal structure of TMP and saDHFR.<sup>12</sup> The docking analyses showed that the diaminopyrimidine (DAP) ring of all derivatives retain key hydrogen bonding interactions with Leu5, Asp27 and Phe92 residues. Interestingly, the methoxy group at *meta*-position of TMP forms a contact interaction with Ser49 side chain. In case of diaveridine, this particular interaction with Ser49 was absent. Halogen-substituted derivative exhibited halogen bonding interaction with Ser49. TMP-I showed strongest halogen bond with 2.28 Å in length, followed by TMP-Cl, and TMP-Br, respectively (see [Supporting information](#)). Interestingly, the trend in halogen bonding strength correlates with the antibacterial potency observed. Hence, the potential interaction of the substituent at the *meta*-position of TMP with Ser49 may affect the antibacterial potency against MSSA and MRSA.

In the treatment of *S. aureus* and MRSA infections, TMP is commonly used in combination with sulfonamide antibiotics such as sulfamethoxazole (SMZ). Such combination exploits the exceptional synergistic effect of the two compounds.<sup>6,7</sup> We, therefore, investigated whether our synthesized halogenated derivatives possess similar synergistic effects with SMZ. Synergistic studies were performed using checkerboard method against reference strain ATCC29213, CA-MRSA strain USA300, and HA-MRSA COL strain. The results were shown in the [Supplementary materials](#). Based on the fractional inhibitory concentration index (FICI), the combination of halogenated TMP and SMZ exhibited synergistic effect with FICI of less than 0.5 (calculated FICI index is in the range of 0.09–0.18) in all strains tested. These excellent

synergistic results were also within the FICI of TMP with SMZ. Note that TMP-I exhibited slightly better synergism with lowest FICI of 0.09 when tested with MSSA control strain. TMP-I could reduce the MIC of SMZ when used in combination up to 30 folds in the case of MSSA and 16 folds in both CA-MRSA and HA-MRSA.

### 3. Conclusion

In conclusion, in this study we incorporated various halogens into trimethoprim structures to exploit the potential halogen bond interactions with saDHFR. The susceptibility of MSSA and global epidemic MRSA USA300 strain SF8300 and COL strains to halogenated TMP derivatives showed high potency in growth inhibitory activity, particularly TMP-I that inhibited growth of all strains with MIC in the range of 1.25–2.5  $\mu\text{g/mL}$ . In comparison to the clinically used antibiotics diaveridine, incorporation of halogen could significantly enhance the ability to inhibit growth of MSSA and MRSA. Similar to TMP, all halogenated TMP could function synergistically with sulfamethoxazole. Interestingly, we observed a trend in potency that correlates to the ability of halogens to participate halogen bonding with Ser49 side chain of the targeted saDHFR binding site. TMP-I was more potent than TMP-Br and TMP-Cl. The binding activity of these halogenated TMP derivatives to saDHFR and the potential role of halogen bond interactions to the protein should be further studied and reported in due course.

### 4. Experimental

#### 4.1. Chemistry

All materials, unless otherwise noted, were obtained from commercial suppliers and used as provided. Reactions were conducted under an inert atmosphere of nitrogen. The progress of reactions was monitored by thin layer chromatography (TLC). <sup>1</sup>H NMR spectra were obtained using either a Bruker DPX-300 (300 MHz), or a Bruker Avance 300, or a Bruker Avance-500 spectrometer. <sup>13</sup>C NMR spectra were obtained using a Bruker Avance-300 spectrometer (75 MHz) spectrometer or a Bruker Avance-500 spectrometer (125 MHz). Chemical shifts were reported relative to residual solvent signals in parts per million ( $\delta$ ) (CDCl<sub>3</sub>: <sup>1</sup>H:  $\delta$  7.27, <sup>13</sup>C:  $\delta$  77.23; DMSO-*d*<sub>6</sub>: <sup>1</sup>H:  $\delta$  2.50, <sup>13</sup>C:  $\delta$  39.51). <sup>1</sup>H NMR data were assumed to be first order with apparent doublets and triplets reported as d and t, respectively. Multiplets were reported as m, and resonances that appear broad were designated as br. High-resolution mass spectra (HRMS) were obtained on a Bruker micro TOF spectrometer in the ESI and/or APCI modes.

#### 4.1.1. Synthesis of halogenated vanillin 1a–1c

4.1.1.1. Synthesis of 3-chloro-4-hydroxy-5-methoxybenzaldehyde (1a). To a solution of vanillin (2.00 g, 13.1 mmol) in glacial acetic

acid (20 mL), *N*-chlorosuccinimide (NCS) (1.76 g, 13.1 mmol) was added. The reaction was stirred at room temperature for 16 h. The reaction was extracted with CH<sub>2</sub>Cl<sub>2</sub>. An organic layer was washed with H<sub>2</sub>O followed by saturated NaCl solution. The resulting organic layer was dried over anhydrous Na<sub>2</sub>SO<sub>4</sub> and concentrated to dryness to afford an off-white solid. The solid was washed with CHCl<sub>3</sub>. Upon filtration, an off-white precipitated crystal product (**1a**) was obtained (1.14 g, 47%). <sup>1</sup>H NMR (300 MHz, DMSO-*d*<sub>6</sub>) δ: 3.89 (s, 3H), 6.45 (s, 1H), 7.38 (d, *J* = 1.77 Hz, 1H), 7.57 (d, *J* = 1.79 Hz, 1H), 9.76 (s, 1H); <sup>13</sup>C NMR (75 MHz, DMSO-*d*<sub>6</sub>) δ: 56.32, 109.16, 120.05, 125.64, 128.18, 148.79, 148.94, 190.49; ESI-MS calc for C<sub>8</sub>H<sub>7</sub>ClNaO<sub>3</sub> [M + Na<sup>+</sup>]<sup>+</sup>: 208.9976, found 208.9975.

**4.1.1.2. Synthesis of 3-bromo-4-hydroxy-5-methoxybenzaldehyde (1b).** To a solution of vanillin (2.00 g, 13.1 mmol) in glacial acetic acid (20 mL), *N*-bromosuccinimide (NBS) (2.57 g, 14.6 mmol) was added. The reaction was stirred at room temperature for 3 h. The reaction was extracted with CH<sub>2</sub>Cl<sub>2</sub>. An organic layer was washed with H<sub>2</sub>O followed by saturated NaCl solution. The resulting organic layer was dried over anhydrous Na<sub>2</sub>SO<sub>4</sub> and concentrated to under vacuum to give an orange to brown solid. The solid was washed with CHCl<sub>3</sub>. An orange crystal of product (**1b**) was filtered and washed with cold CHCl<sub>3</sub> (2.29 g, 75%). <sup>1</sup>H NMR (300 MHz, DMSO-*d*<sub>6</sub>) δ: 4.00 (s, 3H), 6.59 (s, 1H), 7.38 (d, *J* = 1.70 Hz, 1H), 7.65 (d, *J* = 1.71 Hz, 1H), 9.80 (s, 1H); <sup>13</sup>C NMR (75 MHz, DMSO-*d*<sub>6</sub>) δ: 189.66, 148.87, 147.65, 130.06, 129.99, 108.16, 108.00, 56.59; ESI-MS calc for C<sub>8</sub>H<sub>7</sub>BrNaO<sub>3</sub> [M + Na<sup>+</sup>]<sup>+</sup>: 252.9471, found 252.9473.

**4.1.1.3. Synthesis of 3-iodo-4-hydroxy-5-methoxybenzaldehyde (1c).** To a solution of vanillin (0.50 g, 3.29 mmol) in EtOH (70 mL), KI (0.61 g, 3.65 mmol) was added and stirred to mix. The mixture was cooled down to 0 °C with an ice bath. Household bleach solution (CLOROX®) (12.5 mL, equivalent to sodium hypochlorite 8.23 mmol) was added dropwise into the solution mixture. After addition was complete, the reaction was stirred at room temperature for 1 h as EtOH was removed in vacuo. The remaining aqueous solution was neutralized with diluted HCl (1:3 ratio of 1 M HCl to H<sub>2</sub>O). Subsequently, the reaction mixture was extracted with CH<sub>2</sub>Cl<sub>2</sub>. An organic layer was washed with H<sub>2</sub>O followed by saturated NaCl solution, then dried over Na<sub>2</sub>SO<sub>4</sub>. The solution was concentrated to dryness to yield crude product as yellowish solid powder. The powder was washed with CHCl<sub>3</sub>. A white to off-white powder product (**1c**) was obtained upon filtration and washing with cold chloroform (0.74 g, 80%). <sup>1</sup>H NMR (300 MHz, DMSO-*d*<sub>6</sub>) δ: 3.98 (s, 3H), 6.69 (s, 1H), 7.39 (s, 1H), 7.83 (s, 1H), 9.78 (s, 1H); <sup>13</sup>C NMR (75 MHz, DMSO-*d*<sub>6</sub>) δ: 56.19, 84.12, 110.10, 130.00, 134.76, 147.30, 152.20, 190.23; ESI-MS calc for C<sub>8</sub>H<sub>7</sub>I NaO<sub>3</sub> [M + Na<sup>+</sup>]<sup>+</sup>: 300.9332, found 300.9399.

#### 4.1.2. General procedure for methylation of 1a-1c

The methylation reaction of halogenated vanillin derivative (**1a-1c**) were generally conducted based on the previously reported procedure.<sup>19</sup> In brief, into a solution of halogenated vanillin (**1a**, **1b**, or **1c**) (10.17 mmol) in CH<sub>2</sub>Cl<sub>2</sub> (135.0 mL), an aqueous solution of 1.6 M NaOH (75.0 mL) and tetrabutylammonium iodide (TBAI) (15.25 mmol) were added. The reaction was stirred until a clear solution was observed. Methyl iodide (120.5 mmol) was added to a solution mixture and stirred for 16 h at room temperature. The reaction was quenched with 6 M HCl and extracted with CH<sub>2</sub>Cl<sub>2</sub>. The organic layer was subsequently washed with H<sub>2</sub>O followed by saturated NaCl solution. The solution was subsequently dried over Na<sub>2</sub>SO<sub>4</sub> and concentrated to dryness, affording crude product as yellow solid. The crude product was purified by column chromatography to give white solid product **2a-2c**.

**4.1.2.1. 3-Chloro-4,5-dimethoxybenzaldehyde (2a).** White solid product was obtained in 96% yield. <sup>1</sup>H NMR (300 MHz, CDCl<sub>3</sub>) δ: 3.86 (s, 1H), 3.88 (s, 1H), 7.27 (d, *J* = 1.69 Hz, 1H), 7.42 (d, *J* = 1.79 Hz, 1H), 9.76

(s, 1H); <sup>13</sup>C NMR (75 MHz, CDCl<sub>3</sub>) δ: 56.21, 60.92, 109.44, 125.74, 128.84, 132.39, 150.76, 154.31, 189.96; ESI-MS calc for C<sub>9</sub>H<sub>9</sub>ClNaO<sub>3</sub> [M + Na<sup>+</sup>]<sup>+</sup>: 223.0132, found 223.0131.

**4.1.2.2. 3-Bromo-4,5-dimethoxybenzaldehyde (2b).** White solid product was obtained in 98% yield. <sup>1</sup>H NMR (300 MHz, CDCl<sub>3</sub>) δ: 3.86 (s, 3H), 3.88 (s, 3H), 7.31 (d, *J* = 1.76 Hz, 1H), 7.58 (d, *J* = 1.78 Hz, 1H), 9.77 (s, 1H); <sup>13</sup>C NMR (75 MHz, CDCl<sub>3</sub>) δ: 56.24, 60.80, 110.17, 117.92, 128.73, 133.06, 151.83, 154.185, 189.80; ESI-MS calc for C<sub>9</sub>H<sub>9</sub>BrNaO<sub>3</sub> [M + Na<sup>+</sup>]<sup>+</sup>: 266.9627, found 266.9626.

**4.1.2.3. 3-Iodo-4,5-dimethoxybenzaldehyde (2c).** White solid product was obtained in 98% yield. <sup>1</sup>H NMR (300 MHz, CDCl<sub>3</sub>) δ: 3.91 (s, 6H), 7.83 (d, *J* = 1.39 Hz, 1H), 7.83 (d, *J* = 1.53 Hz, 1H), 9.81 (s, 1H); <sup>13</sup>C NMR (75 MHz, CDCl<sub>3</sub>) δ: 56.09, 60.63, 92.09, 111.04, 133.91, 134.67, 152.98, 154.15, 189.68; ESI-MS calc for C<sub>9</sub>H<sub>9</sub>I NaO<sub>3</sub> [M + Na<sup>+</sup>]<sup>+</sup>: 314.9489, found 314.9487.

#### 4.1.3. General procedure for cyclization of 2,4-diamino pyrimidine ring (TMP-Cl, TMP-Br, and TMP-I)

The condensation reactions of halogenated dimethoxy benzaldehyde adducts (**2a**, **2b**, or **2c**) and 3-morpholinopropio nitrile (**3**) were conducted based on the previously reported procedure.<sup>15</sup> Compound **3** (11.49 mmol), prepared based on previously reported procedure.<sup>20</sup> was dissolved in DMSO (3.0 mL) and heated to 65 °C. Into a preheated solution, a freshly prepared sodium methoxide (4.59 mmol) was slowly added and stirred for 45 min at 80 °C. Then, a solution of **2** (9.19 mmol) in DMSO (5.0 mL) was added into the heated solution. The reaction was stirred at 80 °C for 16 h. The reaction was quenched with diluted HCl (1:2 of 1 M HCl in H<sub>2</sub>O) and extracted with CH<sub>2</sub>Cl<sub>2</sub>. An organic layer was subsequently washed with water and saturated NaCl solution. The washed organic layer was dried over Na<sub>2</sub>SO<sub>4</sub>. The solvent was removed under reduced pressure, affording dark brown viscous liquid. The crude product was partially purified by column chromatography to give a yellow to brown viscous liquid mixture. The mixture was carried on to the next step.

The cyclization reactions with guanidine were carried out based on previously reported procedure.<sup>15</sup> In brief, into a solution mixture of guanidine hydrochloride (23.59 mmol) and NaOEt (23.59 mmol) in dry EtOH (6.0 mL), a solution of halogenated dimethoxybenzyl morpholinoacrylonitrile derivative (4.72 mmol) in the mixed solvent of dry EtOH (8.0 mL) and dry DMSO (3.0 mL) was added. The reaction mixture was stirred under refluxing temperature of 80 °C for 16 h. Then, EtOH was removed by rotary evaporation under reduced pressure. The remaining solution was quenched with diluted HCl (1:3 of 1 M HCl in H<sub>2</sub>O). The quenched reaction mixture was extracted with CH<sub>2</sub>Cl<sub>2</sub>. The combined organic layers were washed with H<sub>2</sub>O and saturated NaCl solution, respectively. The resulting solution was dried over Na<sub>2</sub>SO<sub>4</sub>, and concentrated to dryness to obtain crude product as dark brown viscous liquid. The crude product was purified by column chromatography to give partially pure product, which was then further purified by recrystallization in MeOH. The crystal product was washed with 1:1 CH<sub>2</sub>Cl<sub>2</sub>/Hexane to yield the desired product.

**4.1.3.1. 5-(3-Chloro-4,5-dimethoxybenzyl)pyrimidine-2,4-diamine (TMP-Cl).** A light brown crystal product was obtained in 47% yield. <sup>1</sup>H NMR (300 MHz, DMSO-*d*<sub>6</sub>) δ: 3.53 (s, 2H), 3.66 (s, 3H), 3.77 (s, 3H), 5.72 (s, 2H), 6.12 (2, 2H), 6.94 (d, *J* = 1.90 Hz, 1H), 6.96 (d, *J* = 1.88 Hz, 1H), 7.55 (s, 1H); <sup>13</sup>C NMR (75 MHz, DMSO-*d*<sub>6</sub>) δ: 31.95, 55.95, 59.96, 105.17, 112.91, 116.26, 123.40, 138.17, 143.74, 153.07, 156.00, 162.12, 162.35; ESI-MS calc for C<sub>13</sub>H<sub>15</sub>ClN<sub>4</sub>NaO<sub>2</sub> [M + H<sup>+</sup>]<sup>+</sup>: 295.0956, found 295.0954.

**4.1.3.2. 5-(3-Chloro-4,5-dimethoxybenzyl)pyrimidine-2,4-diamine (TMP-Br).** A dark brown crystal product was obtained in 49% yield. <sup>1</sup>H NMR (300 MHz, DMSO-*d*<sub>6</sub>) δ: 3.53 (s, 2H), 3.68 (s, 3H), 3.77 (s, 3H), 5.71 (s,



2H), 6.11 (2, 2H), 6.81 (d,  $J = 1.90$  Hz, 1H), 6.93 (d,  $J = 1.86$  Hz, 1H), 7.55 (s, 1H);  $^{13}\text{C}$  NMR (75 MHz, DMSO- $d_6$ )  $\delta$ : 32.07, 55.97, 60.09, 105.13, 112.24, 120.65, 126.42, 137.54, 142.72, 153.20, 156.06, 162.12, 162.38; ESI-MS calc for  $\text{C}_{13}\text{H}_{15}\text{BrN}_4\text{NaO}_2$   $[\text{M} + \text{H}^+]^+$ : 339.0451, found 339.0453.

**4.1.3.3. 5-(3-Iodo-4,5-dimethoxybenzyl)pyrimidine-2,4-diamine (TMP-D).** A yellow crystal product was obtained in 60% yield.  $^1\text{H}$  NMR (300 MHz, DMSO- $d_6$ )  $\delta$ : 3.51 (s, 2H), 3.63 (s, 3H), 3.75 (s, 3H), 5.70 (s, 2H), 6.10 (2, 2H), 6.96 (d,  $J = 1.81$  Hz, 1H), 7.12 (d,  $J = 1.83$  Hz, 1H), 7.54 (s, 1H);  $^{13}\text{C}$  NMR (75 MHz, DMSO- $d_6$ )  $\delta$ : 31.71, 55.82, 59.76, 92.38, 105.26, 113.81, 129.09, 138.91, 146.34, 151.98, 156.02, 162.12, 162.35; ESI-MS calc for  $\text{C}_{13}\text{H}_{15}\text{IN}_4\text{NaO}_2$   $[\text{M} + \text{H}^+]^+$ : 387.0312, found 387.0301.

#### 4.2. Molecular docking

The molecular docking experiment was performed on Schrödinger Maestro suites using the 'standard protocol'. The saDHFR crystal structure from the Protein Data Bank with co-crystal TMP (PDB ID:2W9H) was refined with Protein Preparation Wizard. The Receptor grid for Glide dock was generated from the refined protein structure and the co-crystal TMP. Ligand structures were constructed from TMP structure and prepared with LigPrep in Schrödinger suites. Glide dock SP was performed with core constrain based on co-crystal TMP. The binding poses from the docking were then subsequently analyzed.

#### 4.3. Microbiology

Overnight bacterial cultures were prepared in Tryptic soy broth (TSB). The susceptibility tests were performed, using Muller-Hinton broth (MHB) supplemented with Bacto Agar. All media were purchased from BD (Sparks, MD). Antibiotics were from Sigma-Aldrich. The trimethoprim-sulfamethoxazole (SXT) disk was purchased from Oxoid (Hampshire, UK).

##### 4.3.1. Bacterial strains and inoculums preparation

A single colony of each strain was picked and transferred into TSB (5 mL) in a sterilized 15-mL test tube, which was then capped and incubated at 37 °C for 16–18 h. The suspension was subsequently diluted in sterilized phosphate buffer saline (PBS) to yield the appropriate inoculum density of approximately  $10^8$  CFU/mL for disk diffusion susceptibility test and  $10^6$  CFU/mL for microdilution assay. The inoculum was used within 15 min after adjusting to its appropriate density.

##### 4.3.2. Disk diffusion

The disk diffusion was performed based on previously reported procedure.<sup>18</sup> Muller-Hinton Agar was sterilized and poured into Petri dishes to acquire 4 mm in thickness. After solidification, bacterial suspension with inoculum density of approximately  $10^8$  CFU/mL were spread on the agar surface using sterile swap. The inoculated plate was let stand at room temperature for 5–10 min before placing a Whatman paper disk (6 mm). Subsequently, a solution of test compound (typically 5  $\mu\text{g}$ , based on suggested breakpoint of TMP, otherwise noted) diluted in DMSO was impregnated onto each paper disk. After 18–20 h of incubation at 37 °C in ambient air incubator, the diameters of inhibition zones were measured in millimeters using sliding callipers. The experiments were performed at least in triplicate.

The zone diameter was measured from the back of the plate. The inhibition zones were classified as complete and incomplete inhibition. The complete zone margin is identified as the area where no obvious visible growth is observed by the naked eyes.

##### 4.3.3. Microdilution assay

The microdilution susceptibility protocol reported by CLSI was used as a guideline.<sup>18</sup> The stock solutions of test compounds at 100 mM in

DMSO were used to prepare series of concentration of each compound by diluting in sterilized Muller-Hinton broth (MHB). An 180  $\mu\text{L}$  aliquot of each compounds at different dilutions was transferred to sterilized 96-well plates. To each aliquot of tested compounds, 20  $\mu\text{L}$  of bacterial inoculum was added to reach final inoculums density of approximately  $10^5$  CFU/mL. The assay plates were incubated at 37 °C for 20 h. After incubation, the optical density of each well was measured using Wallac Victor V1420 Multilable HTS Counter (PerkinElmer, USA). The MIC is determined by the lowest concentration showing no visible growth, quantitatively indicated by the basal optical density. The MBC were determined based on the results obtained from microdilution testings. The solution of well that appeared as clear solution, or quantitatively indicted by basal optical density, was spread on TSA agar plate and subsequently incubated at 37 °C for 18–20 h. The lowest concentration that shows no colony of bacteria is recorded as MBC. The experiments were repeated at least in triplicate.

##### 4.3.4. Cytotoxicity assay

To test cytotoxicity of the synthetic derivatives, we followed previously reported protocol.<sup>21</sup> A549 cells were harvested. Cells (approximately  $10^4$  cells) in 45  $\mu\text{L}$  of DMEM culture medium was added to sterilized 96-well plate. The stock of TMP derivatives tested were prepared by diluting with DMSO. To obtain series of compound tested, the stock solution were subsequently 2-fold diluted with DMEM culture medium. 45  $\mu\text{L}$  of tested compounds in DMEM medium was placed to each well that already contained A549. The assay plate was cultured at 37 °C and 5%  $\text{CO}_2$  incubator for 24–48 h. Subsequently, 10  $\mu\text{L}$  of Prestoblu<sup>®</sup> was added into each well and incubated at 37 °C and 5%  $\text{CO}_2$  for 1 h. Then, the fluorescence intensity of each well was determined using Wallac Victor V1420 Multilable HTS Counter (PerkinElmer, USA). The excitation wavelength was 535 nm and the emission wavelength was 610 nm. Numbers of viable cells were indirectly determined by measuring fluorescent intensity as the dye would transform to fluorescent adduct in viable cells.

##### 4.3.5. Synergy testing by broth microdilution method (Checkerboard Titration)

Checkerboard titration method was performed based on previously reported protocols.<sup>22</sup> In brief, two-fold serial dilutions of our synthetic trimethoprim derivatives and sulfamethoxazole were prepared by diluting in MHB. The range of dilution was chosen to cover the higher end and the lower end of each MIC. 90  $\mu\text{L}$  of each serial dilution of first compound of the combination was dispensed into the successive row, while 90  $\mu\text{L}$  of each serial dilution of second compound was dispensed into the successive column. 20  $\mu\text{L}$  of test strain suspension, of which the inoculum density was adjusted to  $10^6$  CFU/mL, was added. The final inoculum density of each well was approximately  $10^5$  CFU/mL. The plates were incubated at 37 °C for 18 h. After incubation, the optical density of each well was measured. The fractional inhibitory concentration (FIC) and fractional inhibitory concentration index (FICI) calculations were described in the [Supplementary material](#).

#### Acknowledgments

This work was supported in part by the Thailand Research Fund (RSA6180037 grant to C.J.) and the Office of the Higher Education Commission, Mahidol University under the National Research Universities Initiative and the Center of Excellence for Innovation in Chemistry (PERCH-CIC). We would like to thank Professor William R. Roush for allowing access to Schrödinger Maestro suites and James Alburger for assisting in the docking experiment.

#### A. Supplementary data

Supplementary data associated with this article can be found, in the online version, at <http://dx.doi.org/10.1016/j.bmc.2018.05.019>.

## References

1. Otto M. *Annu Rev Microbiol.* 2010;64:143–162.
2. Saini V, Riekerink RG, McClure JT, Barkema HW. *J Clin Microbiol.* 2011;49:1568–1577.
3. Fischbach MA, Walsh CT. *Science.* 2009;325:1089–1093.
4. Melander RJ, Melander C. *ACS Infect Dis.* 2017;3:559–563.
5. Tamma PD, Cosgrove SE, Maragakis LL. *Clin Microbiol Rev.* 2012;25(3):450–470.
6. Masters PA, O'Bryan TA, Zurlo J, Miller DQ, Joshi N. *Arch Intern Med.* 2003;163(4):402–410.
7. Yun MK, Wu Y, Li Z, et al. *Science.* 2012;335:1110–1114.
8. Murima P, McKinney JD, Pethe K. *Chem Biol.* 2014;21:1423–1432.
9. Zander J, Besier S, Ackermann H, Wichelhaus TA. *Antimicrob Agents Chemother.* 2010;54:1226–1231.
10. Huovinen P. *Clin Infect Dis.* 2001;32:1608–1614.
11. Charpentier E, Courvalin P. *Antimicrob Agents Chemother.* 1997;41:1134–1136.
12. Bourne CR, Barrow EW, Bunce RA, Bourne PC, Berlin KD, Barrow WW. *Antimicrob Agents Chemother.* 2010;54:3825–3833.
13. Dale GE, Broger D, D'Arcy A, et al. *J Mol Biol.* 1997;266:23–30.
14. Scholfield MR, Zanden CMV, Carter M, Ho PS. *Protein Sci.* 2013;22(2):139–152.
15. (a) Sirichaiwat C, et al. *J Med Chem.* 2004;47:345–354;  
(b) Nammalwar B, et al. *Eur J Med Chem.* 2012;54:387–396.
16. Tenover FC, Goering RV. *J Antimicrob Chemother.* 2009;64:441.
17. Otto M. *Cell Microbiol.* 2012;14:1513.
18. CLSI. *Performance Standards for Antimicrobial Susceptibility Testing.* CLSI supplement M100 27th ed. Wayne, PA: Clinical and Laboratory Standards Institute; 2017.
19. Bang HB, Han SY, Choi DH, et al. *Synth Commun.* 2009;39(3):506–515.
20. Holcomb WF, Hamilton CS. *J Am Chem Soc.* 1942;64(6):1309–1311.
21. Boncler M, Rózsalski M, Krajewska U, Podsek A, Watala C. *J Pharmacol Toxicol Methods.* 2014;69:9–16.
22. Schwalbe R, Steele-Moore L, Goodwin AC. CRC Press: Boca Raton, FL, 2007; pp 275–298.